CHANSON, H. (2016). "Atmospheric Noise of a Breaking Tidal Bore." *Journal of the Acoustical Society of America*, Vol. 139, No. 1, pp. 12-20 (DOI: 10.1121/1.4939113) (ISSN 00014966).

Atmospheric noise of a breaking tidal bore

by Hubert Chanson ([1])

([1]) The University of Queensland, School of Civil Engineering, Brisbane QLD 4072, Australia

Corresponding author, Email: h.chanson@uq.edu.au

Abstract

A tidal bore is a surge of waters propagating upstream in an estuary as the tidal flow turns to rising and the flood tide propagates into a funnel-shaped system. Large tidal bores have a marked breaking roller. The sounds generated by breaking tidal bores were herein investigated in the field (Qiantang River) and in laboratory. The sound pressure record showed two dominant periods, with some similarity with an earlier study (Chanson 2009, Journal of Acoustical Society of America, Vol. 125, No. 6, pp. 3561-3568, DOI: 10.1121/1.3124781). The two distinct phases were the incoming tidal bore when the sound amplitude increased with the approaching bore, and the passage of the tidal bore in front of the microphone when loud and powerful noises were heard. The dominant frequency ranged from 57 to 131 Hz in the Qiantang River bore. A comparison between laboratory and prototype tidal bores illustrated both common features and differences. The low pitch sound of the breaking bore had a dominant frequency close to the collective oscillations of bubble clouds, which could be modelled with a bubble cloud model using a transverse dimension of the bore roller. The findings suggest that this model might be oversimplistic in the case of a powerful breaking bore, like that of the Qiantang River.

Keywords: Atmospheric noise, Tidal bores, Rumble sound, Qiantang River.

I. INTRODUCTION

A tidal bore is a sharp rise in free-surface elevation propagating upstream in an estuarine system as the tidal flow turns to rising. Also known as aegir, mascaret or pororoca, a tidal bore may form typically during spring tide conditions with tidal ranges exceeding 4 to 6 m when the flood tide converges into a narrow funnelled channel. Figure 1 illustrates the tidal bore of the Qiantang River in China. Figure 2 presents a map of the area. The Tang dynasty poet Liu Yuxi (772-842) described its powerful advance at Yanguan: "In the eighth month, the bore comes roaring in". In a poem, the eminent Song dynasty calligrapher Mi Fu (1052-1107) related the bore arrival: "An angry turbulent sound erupts". A poem by Mei Sheng (9-10th century AD) added: "its angry thunder can be heard a hundred miles; [...] It booms and crashes, like rolls of thunder". In September 1888, Captain Moore observed the Qiantang River bore and summarised his observations: "the sound in the distance is peculiar, and no exactly like any other. It most nearly resembles the leaden noise of breakers on a distant coral reef, being a continuous muttering, broken only by an occasional dull thud,

indicating some new addition to the flood, or some exceptionally heavy breaker. As it approaches, the sound increases very gradually until it passes with a roar, but little inferior to the rapids below Niagara." (Moore, 1888 p. 36). More generally the tidal bore sounds were called a "roar" (Darwin 1897) or a "great destructive noise", often compared to the sound of bass drums and thunder. The Canadian composer Gordon Monahan created a musical piece using sound recordings in the Bay of Fundy: "the tidal bore of the Maccan River" (Monahan 1981). A tsunami bore can also generate a rumble noise as observed in Hawaii in 1960 (Eaton et al., 1961). The rumble noise of tidal bores is known to disorientate animals which would be outrun and drowned by the bore, when they panicked (Chanson, 2011). The acoustic properties of a tidal bore were investigated in the Bay of Mt St Michel (Chanson, 2009). The results suggested that the air bubble entrainment in the tidal bore roller played a major role in the atmospheric noise generation.

The literature on the underwater sounds generated by breaking waves is broad (Lighthill, 1952; Clay and Medwin, 1977; Leighton, 1994; Kerman, 1988; Manasseh et al., 2006). During breaking, the air bubble entrainment, breakup and evolution of the entrained air into numerous bubbles are a source of acoustic noise, causing the ocean ambient noise, and are important for naval hydrodynamics (Prosperetti, 1988; Lamarre and Melville, 1995; Deane, 1997; Carey and Evans, 2011). On another hand, very few studies investigated the atmospheric sound of breaking waves. Low-frequency atmospheric sounds were recorded when waves break against the shoreline (Garces et al., 2006). In a long wave flume, hydrophone, microphone and video records were obtained simultaneously, showing similarities between atmospheric and underwater noise patterns (Kerman, 1987).

Herein, the atmospheric sounds of breaking tidal bores were carefully recorded in the field and in laboratory. The passive acoustic characteristics were analysed and compared to a previous data set. The present work focuses on the acoustic signature of breaking tidal bore processes and the comparative results are discussed in terms of scaling.

II. EXPERIMENTAL CONFIGURATIONS AND MEASUREMENTS

The Hangzhou Bay in China is characterised a large tidal range up to 9 m at the river mouth and fast advancing flood tides. The Bay is drained by a main river: the Qiantang River (Fig. 2A). The Qiantang River catchment area is 49,900 km^2 and its mean annual discharge is 920 m^3/s (Chen et al., 1990). The estuarine zone is 270 km long, of which the downstream 190 km are affected by a major tidal bore (Pan et al., 2007).

Figure 1 presents a number of photographs of the Qiantang River bore in October 2014. Figure 2A shows a dimensioned map with a number of well-known view points. The tidal bore was well documented historically (Moule, 1923; Dai and Zhou, 1987; Chyan and Zhou, 1993). The bore is regarded as very dangerous with numerous warning signs along the estuary banks to stop people wandering near low water. Each year, a number of drownings are reported.

Herein the tidal bore of the Qiantang River was observed at Yanguan, 55 km downstream of the City of Hangzhou, where the river is 2.8 km wide. On the 11 October 2014, photographs were taken during the

daytime bore (Fig. 1 & 2B). Atmospheric sounds were recorded at night with a dSLR Pentax™ K3 equipped with an external Rode™ Stereo VideoMic Pro shotgun on the early morning of 11 and 12 October 2014. The shotgun was equipped with a stereo electret condenser microphone. (The microphone and camera were calibrated afterwards in the anechoic chamber at the University of Queensland.) The camera and microphone were located on a building balcony on 11 October 2014 and near the edge of the old seawall on 12 October 2014 (Fig. 2C). Their location was fixed for each record but the microphone was aimed towards the tidal bore front for the whole duration of the records. The recording on 11 October data set was a test, consisting of a short data set taken in less than optimum conditions. The sound record on 12 October was conducted with greater care and, in particular, the microphone location was more appropriate. In each case, the microphone was fixed to the camera's hotshoe. Its maximum sound pressure level was 134 dB and the SNR setting was 74dB. The audio signal (PCM digital sound: 16 bit, 48 kHz, 2 channels) was separated from the video signal. The signal was digitized at 48 kHz, implying a Nyquist frequency of about 24 kHz. The .WAV recordings were processed with the software DPlot™ version 2.3.5.3. Fast Fourier transforms (FFTs) were taken. Each experimental data set was sub-sampled into sub-sets 5 s long to give a frequency span of 0-24 kHz.

Similarly, sound recordings were conducted with the same equipment in a 19 m long 0.7 m rectangular channel located at the University of Queensland. An initially steady flow was set and the tidal bore was generated by the rapid and complete closure of a downstream gate (Leng and Chanson, 2015). The bore sound was recorded 9 m upstream of the gate. The sound recording was started a few seconds after the gate closure and stopped before the bore reached the channel's upstream end. The overall record was relatively short. Hence the experimental data set was sub-sampled into sub-sets 0.2 s long. Figure 3 shows some photographs of the breaking bore and Table I summarises the main flow conditions.

Remark

Both field and laboratory data sets indicated some sound energy between 5 and 30 Hz, irrespective of the time and of the proximity of the tidal bore. Some complementary test with the same camera and microphone was performed at night with minimum background noise with (a) the shotgun mounted on the camera hotshoe and (b) the shotgun placed 20 cm away from the camera body. All the camera settings were otherwise identical for all tests. The records were sub-sampled and analysed identically to the field data sets. The results (not shown) indicated a marked difference in sound energy at low frequency (10-30 Hz), suggesting that the microphone mounted on the hotshoe picked up some low-frequency noise within the camera body. This might be linked to the servos that move the sensor during active in-camera shake reduction and hold the sensor still when the mirror is up. In the following, the data analyses will focus on the signal frequencies above 30 Hz.

CHANSON, H. (2016). "Atmospheric Noise of a Breaking Tidal Bore." *Journal of the Acoustical Society of America*, Vol. 139, No. 1, pp. 12-20 (DOI: 10.1121/1.4939113) (ISSN 00014966).

III. PHYSICAL OBSERVATIONS

A. Field observations

On 11 and 12 October 2014, the tidal bore of the Qiantang River was observed in the early morning darkness about 5 hours before sunrise as well as on the 11 October midday when the sky was overcast. The bore arrived as a single line, guided by the northern seawall (Fig. 1B & 2B). The bore front passed in front of the microphone before impacting onto the research station at 01:06 on 11 October morning and 01:34 on 12 October morning. Note that all times are given as local times (UTC + 8 hours). After crashing on the research station platform, the tidal bore continued upstream towards Hangzhou. During daytime on 11 October, the author followed the bore from Xinchang at 12:57, to Yanguan at 13:28, to Laoyanchang at 14:00, up to Jiuxi at 15:30 (see locations in Fig. 2a). The entire process was a breaking bore during all observations (Fig. 1). At night, the white waters of the bore roller were seen with the embankment lighting, but there was not enough light for high-speed photographic observations.

On 11 October, the sound measurements started at 01:04 and lasted for about a minute as the bore passed in front of the research station. On 12 October, the bore was heard since 01:00, and the record started at 01:23, lasting till 01:35 (Fig. 4). The entire bore sound record may be sub-divided into two distinct periods. From the first part of the record, the tidal bore approached Yanguan and the sound amplitude increased gradually up to t = 5480 s. For 5480 s < t, the bore approached the recording location in a very loud manner, dominated by the bore impact and reflection on the old seawall (Fig. 2A). At t = 5634 s, the tidal bore passed in front of the microphone with a celerity about 4.35 m/s, and later "crashed" onto the platform at t = 5654 s, with loud and powerful noises. For 5654 < t < 6543 s, the tidal bore continued upstream towards Laoyanchang and Hangzhou, and the audio record was a combination of the sounds generated by the advancing tidal bore in the background, the flood tidal flow past the research station platform and the flood flow past the old seawall in the foreground. The entire sound pressure record is presented in Figure 4A and the time of passage of the bore is listed in the figure caption.

The sound record characteristics were analysed in terms of the sound pressure amplitude. The results are summarised in Table II (columns 5 and 6), in terms of the mean and standard deviation of the sound pressure modulus. On 12 October, the author stood on the top of the seawall on 12 October. The mean sound pressure modulus data showed an increasing amplitude with the approaching bore. For t < 5480 s, the experimental data were matched closely with a simple source model (Lighthill, 1978; Moser, 2009), in which the sound pressure is proportional to $(x^2+h^2)^{-1/2}$, with x the longitudinal distance parallel to the seawall between the bore front and microphone location and h the microphone's vertical elevation above the initial water level: h ≈ 6 m. It is acknowledged that a line source model might give slightly better results, especially at far distances. During the second period (5480 < t < 6543 s), the sound levels were in average 50% louder than during the first period (incoming bore) (Fig.4B). The mean sound levels reached more than 50 dB about the bore passage in front of the microphone, with maximum sound pressure modulus up to 40 Pa. (The sound level L_p and sound pressure P are related as: $L_p = 20 \log_{10}(P) + 94$ (Hansen 2001).) The quantitative data

were consistent with the personal observations during the tidal bore. The ratio of standard deviation to mean pressure modulus value was typically between 8 and 12 for all observations, independently of the period (Table II).

A spectral analysis of the sound record was conducted, and the basic properties are summarised in Table II (columns 7 and 8). The sound pressure spectra are presented in Figure 5 for several time periods encompassing the two characteristic periods of the sound record presented in Figure 4. Ignoring the signal frequencies below 30 Hz (see discussion above), each spectrum exhibited a dominant frequency with the characteristic values summarised in Table II (column 7). The dominant frequency ranged from 57 to 131 Hz depending upon the time. During the first period of the record ($t < 5480$ s), the dominant frequencies were within 57-62 Hz. Such values corresponded to a low pitch rumble sound, and the rumble frequency was linked to collective oscillations of bubble clouds entrapped in the bore roller (Prosperetti, 1988; Kolaini et al., 1994). The breaking bore advanced rapidly in the main channel (Fig. 1). The low-frequency sound (57-62 Hz) was a characteristic feature of the breaking roller, caused by the turbulence and entrained bubbles in the roller.

For the second characteristic period ($t > 5480$ s), the tidal bore impacted onto the seawall and the impact was an energetic process generating louder noises of a higher pitch, yielding a dominant frequency around 131 Hz. The noise levels were high including when the bore crashed into the research station platform. This is seen in Figure 4 where the higher acoustic energy illustrated a louder noise, as well as in Figure 5 with a larger integral of the power spectral density (PSD) function (Table II, column 8). Note that, since all peak frequencies were greater than the low-frequency in-camera noise found below 30 Hz, no high-pass filtering was required.

B. Laboratory observations

In the laboratory, the sound record focused on the incoming bore and the data were relatively short. The bore arrived as a two-dimensional breaking roller guided by the glass sidewalls of the rectangular channel (Fig. 3). The bore front passed directly beneath the microphone before continuing further upstream. The entire record contained relatively loud noises. A first phase of increasing sound pressure amplitude was not observed, likely the result of a combination of relatively short record and ambient noise in the laboratory.

A spectral analysis of the record was conducted. A typical acoustic spectrum is shown in Figure 6 and basic properties are summarised in Table II. Ignoring the low frequencies (see above), the data exhibited a dominant frequency with the characteristic values summarised in Table II (column 7). The dominant frequency ranged from 220 to 732 Hz.

C. Comments

The acoustic signature of the tidal bore event was compared with an earlier sound record (Chanson, 2009). That of the breaking tidal bore of the Sélune River at the Pointe du Grouin du Sud in October 2008 at night

(Table I). The present data record showed two distinctive periods, with the approaching bore, and the bore passage in front of Yanguan. (No third period was noted contrarily to the observations of Chanson (2009), possibly because the noise of the flood flow on the research station dominated the sound record.) In both set of observations, the sound recording was conducted in the middle of the night in absence of spectators; this feature guaranteed a minimum level of background noise for a better characterisation of the bore acoustic properties. The time development of the audio amplitude was somehow comparable to that of breaking waves observed in laboratory (Kerman, 1987), although with a considerably longer time scale. Namely a time scale of the sound envelop of about 10^3 s for the tidal bore, compared to 10^0 s for breaking waves (Kerman, 1987).

The acoustic spectra of the sound pressure record are presented in Figure 5 for five segments: the first two corresponding to the approaching bore and the last three for the bore passage in front of the research station. The comparison is relevant since all the sound data were recorded with the same microphone from the same location. In Figure 5, the plots illustrate the minimum in energy at roughly 30 Hz for all data. Above maxima were observed for frequencies between 56 and 131 Hz. While all data sets corresponded to low-frequency noises, the loudness of the tidal bore propagation along the seawall and its crashing onto the research station platform is highlighted by its high acoustic energy (Fig. 6, $t > 5480$ s).

The Qiantang River and Sée-Sélune River tidal bores exhibited similar acoustic features during the first period of each record (Fig. 4). First the sound amplitude increased with increasing time as the bore propagated upstream towards the microphone. Second the sound level was much lower and less energetic than during the subsequent record section. The acoustic spectra of the Sée-Sélune River and Qiantang River tidal bores showed some low-pitch sound frequency, the Sée-Sélune River tidal bore having a slightly higher dominant frequency (76-77 Hz) than that of the Qiantang River tidal bore (Table II, column 7).

There were however a number of key differences between the two tidal bore events. While both tidal bores were breaking bores with a marked roller, the Qiantang River tidal bore propagation was constrained by the seawall. Since the sound amplitude falls off as $1/r$, and the sound power as $1/r^2$, where r is the radial distance to the microphone, sounds generated in the vicinity of the recording device contributed most to the measured sound and this included the bore crashing on the seawall slope. Further the Qiantang River bore roller was massive ($\Delta d \approx 3.0$ m) with intense turbulence and air bubble entrainment, and its passage in front of the microphone was associated with the impact onto a man-made platform. Thus the interactions of the bore and flood flow with man-made structures induced loud noises which dominated the second part of the acoustic record (Fig. 4, $t > 5654$ s).

IV. DISCUSSION

In a breaking bore, large scale eddies are generated at the roller toe and advected downstream (Yeh and Mok, 1990; Hornung et al., 1995; Leng and Chanson, 2015). The generation, growth, advection, and pairing of the vortical structures are responsible for low-frequency oscillations of the turbulent velocity field in the bore

roller (Long et al., 1991, Chanson and Gualtieri, 2008; Wang and Chanson, 2015). The breaking bores are also characterised by some air bubble entrainment at the roller toe and advection in the roller (Leng and Chanson, 2015) (Fig. 3A). Figure 3A shows the air bubble entrapment in the roller shear region in laboratory. For a breaking tidal bore (Fig. 1 and 3), the common dimensions of the bubbly flow region are the roller height ($\Delta d = d_2$-d_1), the streamwise bubbly flow length L_{air} that would be the horizontal length of the whole bubble cloud in Figure 3A, and the roller toe perimeter L. Laboratory experiments in moving breaking bores and stationary hydraulic jumps showed that the ratio of (horizontal) bubble cloud length to roller height varied with the Froude number, yielding on average:

$$\frac{L_{air}}{d_2 - d_1} = 19.75\,(Fr_1 - 1)^{0.757} \qquad 1.5 < Fr_1 < 13 \quad (1)$$

Equation (1) is compared with experimental data in Figure 7. Lastly the roller toe perimeter L_p was about 2.8 km at Yanguan.

The resonance frequency of an underwater bubble cloud is lower than that of individual bubbles (Leighton, 1994; Deane, 1997). For a spherical cloud of bubbles, the resonance frequency of the cloud may be derived from the modified Minnaert formula (Carey and Evans, 2011):

$$F = \frac{1}{2\pi R_b}\sqrt{\frac{3\,P}{\rho\,\alpha(1-\alpha)}} \quad (2)$$

where R_b is the bubble cloud radius, P is the ambient pressure, ρ is the fluid density and α is the void fraction. For an idealised spilling breaker, Prosperetti (1988) proposed in first approximation the lowest natural frequency of the bubble cloud as:

$$F = \frac{1}{L_p}\sqrt{\frac{P}{\rho\,\alpha}} \quad (3)$$

where L_p is the length of the breaking roller, more explicitly the roller toe perimeter length. The definition of the cloud dimension is not trivial for a breaking tidal bore because the bore roller is a highly three-dimensional bubbly flow region. Recent observations showed the transverse variation of instantaneous toe perimeter presented some pseudo-periodic fluctuations sketched in Figure 8. These toe perimeter oscillations were observed in both the Qiantang River (2013 field data) and present laboratory facility. The data indicated a range of perimeter wavelengths within $0.7 < L_w/d_1 < 25$, with the two dominant dimensionless wave length ranges being $L_w/d_1 = 1$ and 5-10 (Leng and Chanson, 2015). It is believed that these features were evidences of streamwise vortices and streaks, somehow similar to those observed in plane mixing layers and wall jets. Physically the transverse vortical structures may control the air entrapment in the roller, and the toe perimeter wave length L_w is considered a representative length scale of the bubble cloud length. Thus the lowest natural frequency of a transverse structure of length L_w becomes:

$$F = \frac{1}{L_w}\sqrt{\frac{P}{\rho\,\alpha}} \quad (4)$$

Equation (4) implies that large tidal bores would generate lower pitch sound than small ones. Considering the Qiantang River bore at Yanguan (Fig. 1C) and assuming $L_w/d_1 = 1$, the lowest natural frequency of the bubbly cloud would be about 40-50 Hz for 1% void fraction, close to present observations (Table II). The result tends to suggest that the air bubbles entrapped in the large-scale structures of the tidal bore roller might be acoustically active and contribute to the rumble sound generation.

Figure 9 presents a comparative summary of the dominant frequencies of tidal bore rumble frequency in the field and in laboratory. The data are compared with Equation (4) assuming $L_w/d_1 = 1$. Overall the comparison shows that the sounds generated by the breaking bore had a low-pitch comparable to the sound generated by collective oscillations of rising bubble clouds. The low rumble frequency may explain the general public's perception of approaching breaking bores as galloping horses and locomotive trains. While Equation (4) provided some reasonable estimate for both laboratory and Sée-Sélune River sound frequency data, Figure 9 tends to suggest that it might be oversimplistic in the case of the Qiantang River bore.

V. CONCLUSION

The atmospheric sounds generated by the breaking tidal bore of the Qiantang River were carefully documented in October 2014. The sound record showed two dominant periods, with some similarity during another tidal bore event in the Sée-Sélune River. Similar features includes: (a) the incoming tidal bore phase when the sound amplitude increased with the approaching bore front and air entrapment in the bore roller plays a major role in terms of acoustic signature, and (b) the passage of the tidal bore in front of the microphone where the impacts of the bore on the bank or platform generated loud and powerful noises. The distinction between periods was easily heard in situ.

During the first period, the tidal bore sounds were generated by the bore front hydrodynamic processes including turbulence, air entrainment and breaking next to the bank. The dominant sound frequency ranged between 57 and 131 Hz in the Qiantang River bore. A comparison between laboratory and prototype tidal bores illustrated both common features and differences. The low pitch rumble of the breaking bore had a dominant frequency close to the collective oscillations of bubble clouds, and the air entrapment in the bore roller was likely the major factor in the acoustic signature of the bore. Both laboratory and Sée-Sélune River sound frequency data were successfully modelled with a bubble cloud model based a characteristic transverse dimension of the roller (Eq. (4)). The results suggest that the bubbles entrapped in large-scale structures of the bore roller might be acoustically active and contribute to the rumble sound generation. Yet the findings hint that this model might be simplistic in the case of the Qiantang River bore.

ACKNOWLEDGMENTS

The author thanks Prof Dong-Zi Pan, Zhejiang Institute of Hydraulics and Estuary (China) for the helpful assistance. The assistance of Ms Xinqian Leng, the University of Queensland (Australia) with the laboratory

CHANSON, H. (2016). "Atmospheric Noise of a Breaking Tidal Bore." *Journal of the Acoustical Society of America*, Vol. 139, No. 1, pp. 12-20 (DOI: 10.1121/1.4939113) (ISSN 00014966).

experiments is acknowledged. The author is most grateful of the hospitality of Professor Youcheng Xu at the research station of the Qiantang River Administration of Zhejiang Province (China). The financial support of the Zhejiang Institute of Hydraulics and Estuary and of the University of Queensland is acknowledged.

REFERENCES

Carey, W.M., and Evans, R.B. (**2011**). *Ocean ambient noise: Measurement and theory*. Springer, New York, USA, pp. 1-263.

Chanson, H. (**2009**). "The Rumble Sound Generated by a Tidal Bore Event in the Baie du Mont Saint Michel. " *Journal of Acoustical Society of America*, **125**(6), 3561-3568 (DOI: 10.1121/1.3124781).

Chanson, H. (**2010**). "Convective Transport of Air Bubbles in Strong Hydraulic Jumps." *International Journal of Multiphase Flow*, **36**(10), 798-814 (DOI: 10.1016/j.ijmultiphaseflow.2010.05.006).

Chanson, H. (**2011**). *Tidal Bores, Aegir, Eagre, Mascaret, Pororoca: Theory and Observations*. World Scientific, Singapore, pp. 1-220.

Chanson, H., and Gualtieri, C. (**2008**). "Similitude and Scale Effects of Air Entrainment in Hydraulic Jumps." *Journal of Hydraulic Research*, IAHR, **46**(1), 35-44.

Chen, J., Liu, C., Zhang, C., and Walker, H.J. (**1990**). "Geomorphological Development and Sedimentation in Qiantang Estuary and Hangzhou Bay." *Journal of Coastal Research*, **6**(3), 559-572.

Chyan, S., and Zhou, C. (**1993**). *The Qiantang Tidal Bore*. Hydropower Publ., Beijing, China, The World's Spectacular Sceneries, pp. 1-152 (in Chinese).

Clay, C.S., and Medwin, H. (**1977**). *Acoustical oceanography: principles and applications*. John Wiley, New York, USA, pp. 1-544.

Dai, Z., and Zhou, C. (**1987**). "The Qiantang Bore." *International Journal of Sediment Research*, **1**, 21-26.

Darwin, G.H. (**1897**). *The Tides and Kindred Phenomena in the Solar System*. Lectures delivered at the Lowell Institute, Boston, pp. 59-73 (Reprinted: W.H. Freeman and Co. Publ., London, 1962).

Deane, G. (**1997**). "Sound generation and air entrainment by breaking waves in the surf zone." *Journal of the Acoustical Society of America*, **102**(5), 2671-2689 (DOI: 10.1121/1.420321).

Eaton, J.P., Richter, D.H., and Ault, W.U. (**1961**). "The tsunami of May 23, 1960, on the Island of Hawaii." *Bulletin of the Seismological Society of America*, **51**(2), 135-177.

Garces, M., Aucan, J., Fee, D., Caron, P., Merrifield, M., Gibson, R., and Bhattacharyya, J. (**2006**). "Infrasound from large surf." *Geophysical Research letters*, **33**, L05611, 4 pages (DOI: 10.1029/2005GL025085).

Hansen, C.H. (**2001**). "Chapter 1: Fundamentals of Acoustics." In *Occupational Exposure to Noise: Evaluation, Prevention and Control*. World Health Organisation Special Report, S64. Federal Institute of Occupational Safety and Health, Germany, pp 1-52.

Hornung, H.G., Willert, C., and Turner, S. (**1995**). "The Flow Field Downstream of a Hydraulic Jump." *Journal of Fluid Mechanics*, **287**, 299-316.

CHANSON, H. (2016). "Atmospheric Noise of a Breaking Tidal Bore." *Journal of the Acoustical Society of America*, Vol. 139, No. 1, pp. 12-20 (DOI: 10.1121/1.4939113) (ISSN 00014966).

Kerman, B.R. (**1988**). *Sea Surface Sound - Natural mechanisms of surface generated noise in the ocean*. Kluwer, Dordrecht, Germany, pp. 1-639.

Kerman, B.R. (**1987**). "Audio Signature of a Laboratory Breaking Wave." *Proc. NATO Advanced Research Workshop on Sea Surface Sound*, Lerici, Italy, 15-19 June, NATA ASI Series C, Mathematical and Physical Sciences, 238, 12 pages. (Also in Kerman, B.R. 1988. *Sea Surface Sound*, Kluwer, 437-448)

Kolaini, A.R., Roy, R.R., and Gardner, D.L. (**1994**). "Low-Frequency Acoustic Emissions in Fresh and Salt Water." *Journal of Acoustic Society of America*, **96**(3), 1766-1772.

Lamarre, E., and Melville, W.K. (**1995**). "Instrumentation for the measurement of sound speed near the ocean surface." *Journal of Atmospheric and Oceanic Technology*, **12**(2), 317-329.

Leighton, T.G. (**1994**). *The acoustic bubble*. Academic Press, San Diego, USA, pp. 1-613.

Leng, X., and Chanson, H. (**2015**). "Turbulent Advances of a Breaking Bore: Preliminary Physical Experiments." *Experimental Thermal and Fluid Science*, **62**, 70-77 (DOI: 10.1016/j.expthermflusci.2014.12.002).

Lighthill, M.J. (**1952**). "On sound generated aerodynamically I- General theory." *Proceedings of Royal Society of London*, Series A, **211**(1107), 564-587.

Lighthill, J. (**1978**). *Waves in Fluids*. Cambridge University Press, Cambridge, UK, pp. 175-181.

Long, D., Rajaratnam, N., Steffler, P.M., and Smy, P.R. (**1991**). "Structure of Flow in Hydraulic Jumps." *Journal of Hydraulic Research*, IAHR, **29**(2), 207-218.

Manasseh, R., Babanin, A.V., Forbes, C., Rickards, K., Bobevski, I, and Ooi, A. (**2006**). "Passive acoustic determination of wave-breaking events and their severity across the spectrum." *Journal of Atmospheric and Oceanic Technology*, **23**(4), 599-618.

Monahan, G. (**1981**). "The tidal bore of the Maccan river." *Musical piece* (URL: http://www.gordonmonahan.com/pages/tidal_bore.html, last viewed 18/8/15).

Moore, R.N. (**1888**). *Report on the Bore of the Tsien-Tang Kiang*. Hydrographic Office, London, pp. 7-37.

Moser, M. (**2009**). *Engineering Acoustics. An Introduction to Noise Control*. Springer, Dordrecht, Germany, 2nd edition, pp. 67-110.

Moule, A.C. (**1923**). "The Bore on the Ch'ien-T'ang River in China." *T'oung Pao*, Archives pour servir à l'étude de l'histoire, des langues, la geographie et l'ethnographie de l'Asie Orientale (Chine, Japon, Corée, Indo-Chine, Asie Centrale et Malaisie), **22**, 10-188.

Pan, C.H., Ling, B.Y., and Mao, X.Z. (**2007**). "Case study: Numerical modeling of the tidal bore on the Qiantang River, China." *Journal of Hydraulic Engineering*, ASCE, **133**(2), 130-138.

Prosperetti, A. (**1988**). "Bubble-Related Ambient Noise in the Ocean." *Journal of Acoustic Society of America*, **84**(3), 1042-1054.

Rajaratnam, N. (**1962**). "An Experimental Study of Air Entrainment Characteristics of the Hydraulic Jump." *Journal of Institution of Engineers India*, **42**(7), 247-273.

Wang, H., and Chanson, H. (**2015**). "An Experimental Study of Turbulent Fluctuations in Hydraulic Jumps." *Journal of Hydraulic Engineering*, ASCE, **141**(7), Paper 04015010, 10 pages (DOI:

CHANSON, H. (2016). "Atmospheric Noise of a Breaking Tidal Bore." *Journal of the Acoustical Society of America*, Vol. 139, No. 1, pp. 12-20 (DOI: 10.1121/1.4939113) (ISSN 00014966).

10.1061/(ASCE)HY.1943-7900.0001010).

Yeh, H.H., and Mok, K.M. (**1990**). "On Turbulence in Bores." *Physics of Fluids A*, **A2**(5), 821-828.

Tables

Table I - Experimental conditions for the acoustic measurements of breaking tidal bore sounds

Reference	Tidal bore	d_1 (m)	U (m/s)	d_2-d_1 (m)	Fr_1	Remarks
(1)	(2)	(3)	(4)	(5)	(6)	(7)
Present study	Qiantang River, 11 Oct. 2014	2-2.5	4.35	3	2	At Yanguan (left bank)
	Laboratory experiment	0.1055	0.66	0.19	2.3	University of Queensland
Chanson (2009)	Sélune River, 15 Oct. 2008	0.35-0.5	--	0.7-1	2.45	At Pointe du Grouin du Sud (right bank)

Notes: d_1: initial flow depth; Fr_1: bore Froude number; U: bore celerity; d_2-d_1: bore roller height.

CHANSON, H. (2016). "Atmospheric Noise of a Breaking Tidal Bore." *Journal of the Acoustical Society of America*, Vol. 139, No. 1, pp. 12-20 (DOI: 10.1121/1.4939113) (ISSN 00014966).

Table II - Acoustic properties of tidal bore atmospheric sound records

Reference	Record	Duration (s)	Audio track	Average sound pressure modulus (Pa)	STD sound pressure modulus (Pa)	Dominant frequency (range) (*) (Hz)	Integral of PSD function [40Hz-20 kHz] (*) (Pa^2)	Remarks
(1)	(2)	(3)	(4)	(5)	(6)	(7)	(8)	(9)
Qiantang River tidal bore, 11 Oct. 2014	**Tidal bore (breaking)**							At Yanguan (left bank)
	3551	26	Left	--	--	60.1 (45-65)	--	Bore passage
			Right	--	--	60.1 (45-65)	--	
Qiantang River tidal bore, 12 Oct. 2014	**Tidal bore (breaking)**							At Yanguan (left bank)
	4166C	105	Left	0.00359	0.02847	66.7 (65-70)	0.1738	Incoming tidal bore
			Right	0.00358	0.02801	66.7 (65-70)	0.17138	
	4167A	140	Left	0.00574	0.06697	61.9 (55-85)	0.3481	Incoming tidal bore
			Right	0.00572	0.06683	61.9 (55-85)	0.3437	
	4167B	132	Left	0.01922	0.15649	131.1 (70-155)	6.066	Bore passage & Bore crashing on research station
			Right	0.01906	0.15353	131.1 (70-155)	5.947	
Laboratory experiment	**Breaking bore**							
		1.5	Left	0.00999	0.03729	228 & 527 (180-600)	7.581	Run 1
			Right	0.00993	0.03678	228 & 527 (180-600)	7.472	
		1.2	Left	0.02099	0.05637	220, 533 & 732 (180-750)	10.183	Run 2
			Right	0.02088	0.05617	220, 533 & 732 (180-750)	10.183	

Notes: Modulus = absolute value; PSD = power spectral density; STD = standard deviation; (*): field data set sub-sampled into sub-sets 5 s long and averaged; laboratory data set sub-sampled into 0.2 s long sub-sets and averaged.

CHANSON, H. (2016). "Atmospheric Noise of a Breaking Tidal Bore." *Journal of the Acoustical Society of America*, Vol. 139, No. 1, pp. 12-20 (DOI: 10.1121/1.4939113) (ISSN 00014966).

Figures

Fig. 1 - Photographs of the tidal bore of the Qiantang River (China) on 11 October 214

(a) Breaking bore between Xinchang and Qilimiao on 11 October 2014 about 13:10

(b) Tidal bore at Yanguan on 11 October 2014 at 13:28 - The bore front was 3 m high

Fig. 1 - Photographs of the tidal bore of the Qiantang River (China) on 11 October 214

(c) Bore between Yanguan and Laoyanchang about 13:47

(d) Breaking bore at Juixi about 15:30

Fig. 2 - Estuarine zone of the Qiantang River (China) affected by the tidal bore

(a) Dimensioned map of the estuarine zone of the Qiantang River affected by a tidal bore

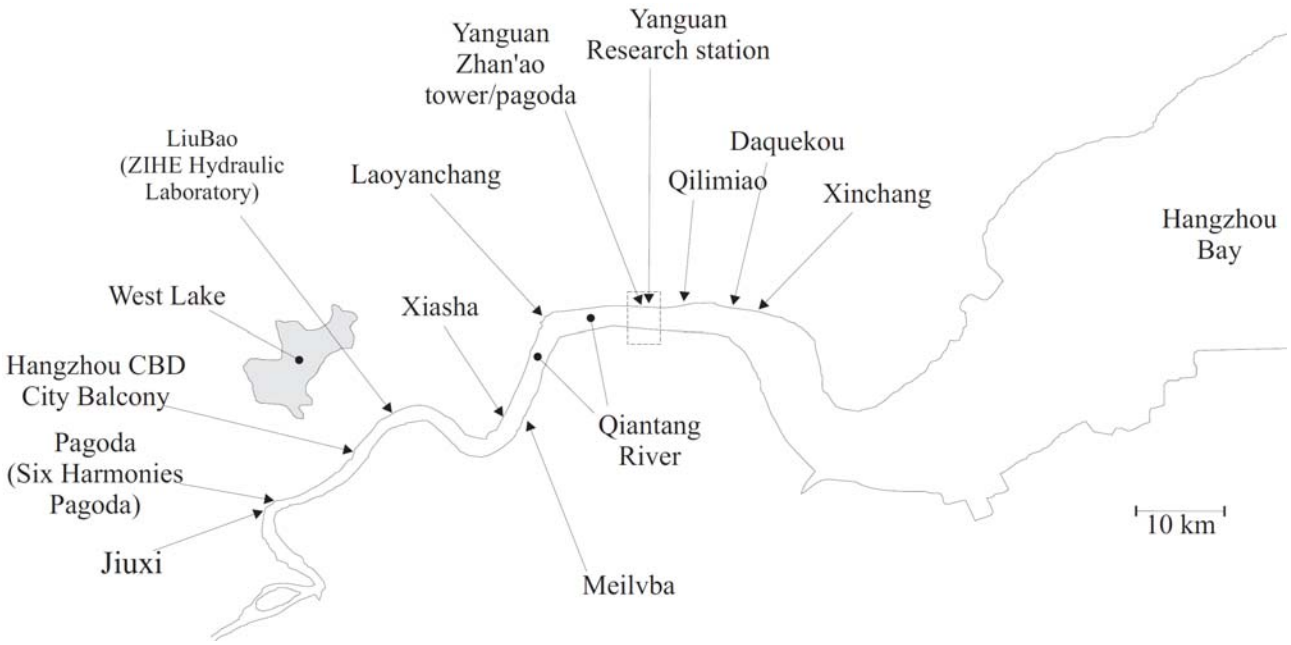

(b) Detailed sketch of Yanguan, viewed in elevation

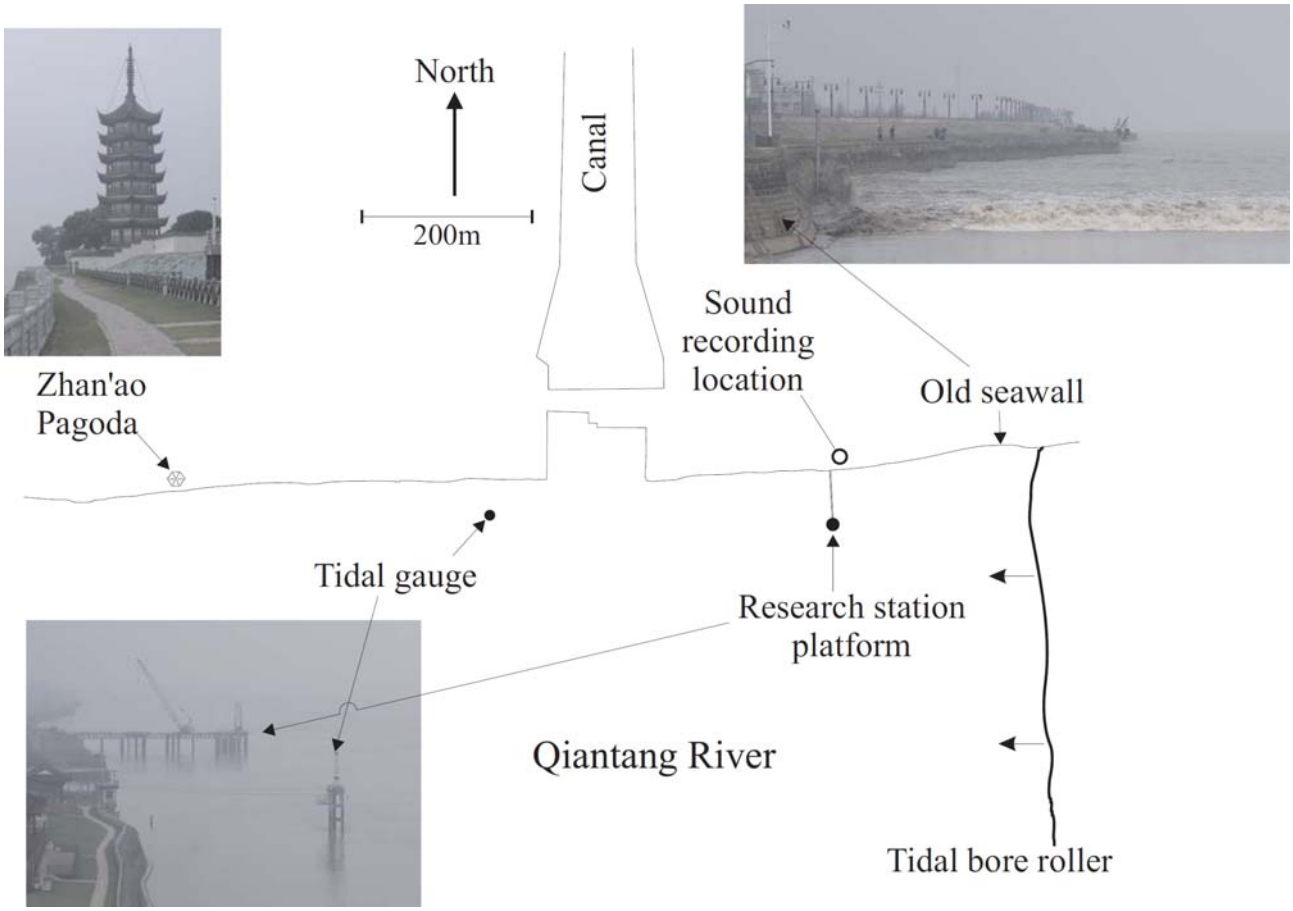

390 Fig. 2 - Estuarine zone of the Qiantang River (China) affected by the tidal bore

391 (c) Undistorted cross-sectional sketch of sound recording locations on 11 and 12 October 2014

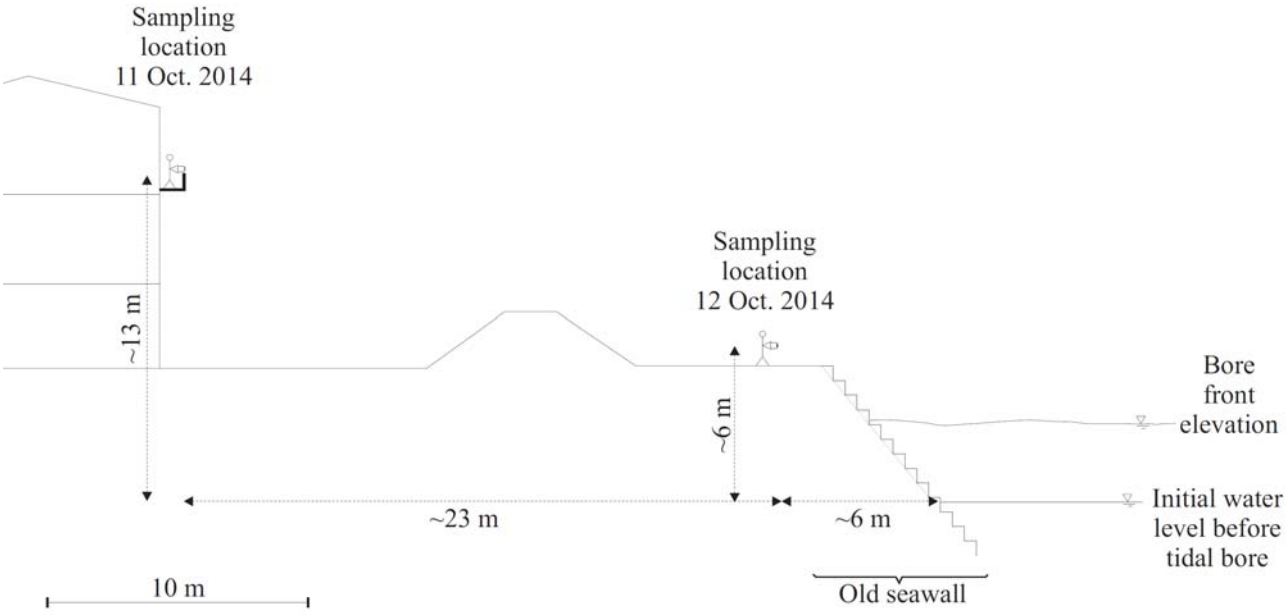

392

393

394

CHANSON, H. (2016). "Atmospheric Noise of a Breaking Tidal Bore." *Journal of the Acoustical Society of America*, Vol. 139, No. 1, pp. 12-20 (DOI: 10.1121/1.4939113) (ISSN 00014966).

Fig. 3 - Photographs of the laboratory breaking bore (shutter speed: 1/2,000 s)

(a) Sideview with bore propagating from right to left

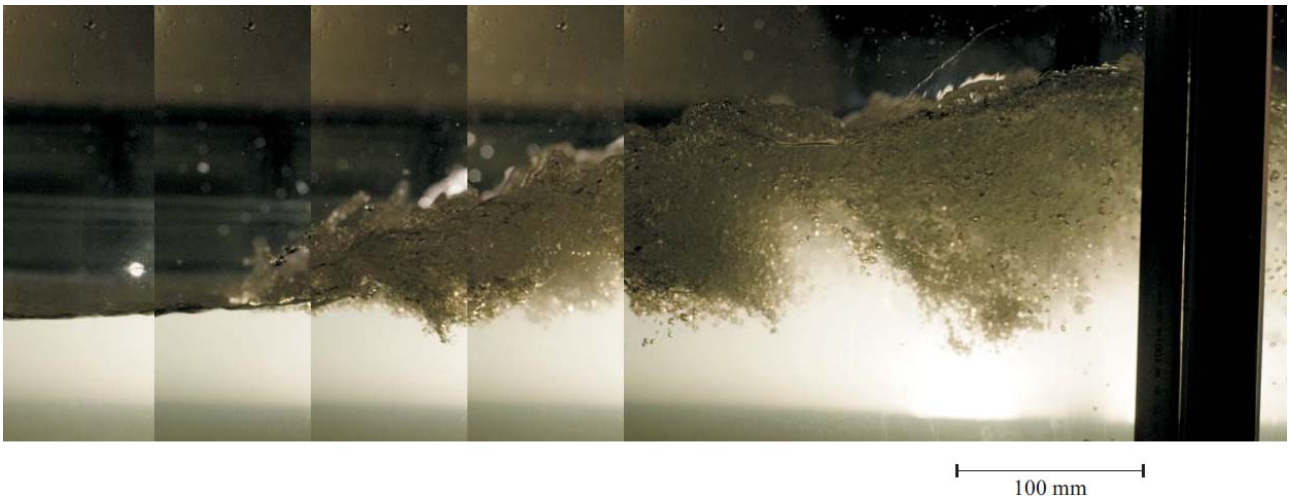

(b) Looking downstream at the incoming breaking bore roller

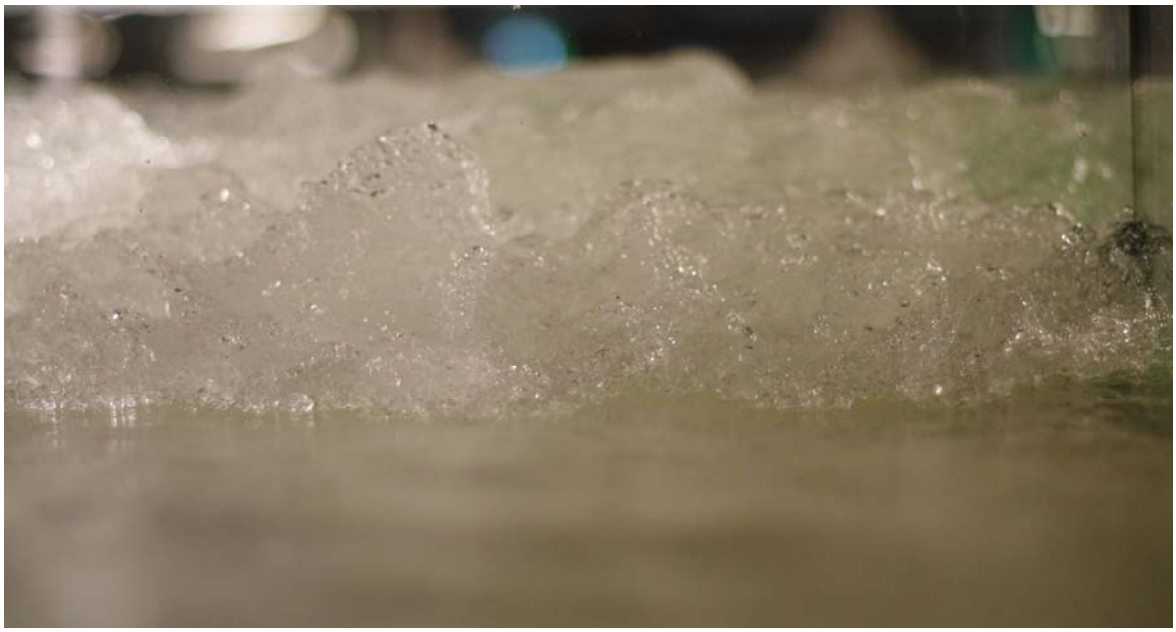

Fig. 4 - Sound record of the tidal bore of the Qiantang River at Yanguan on 12 October 2014 between 01:22 and 01:42 - The bore front passed in front of the microphone at 01:33:54 (t = 5634 s) and impacted onto the research station platform at 01:34:14 (t = 5654 s) - Solid line demarks two distinctively different periods (a) Time variation of the sound pressure in Pascals - Dashed lines show the envelop trend

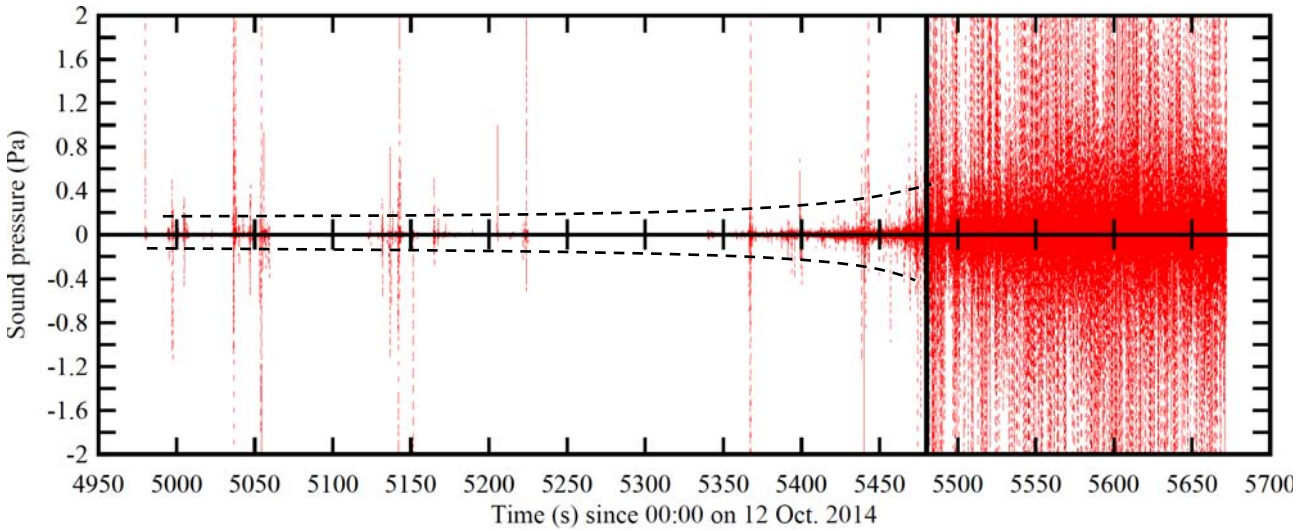

(b) Time variation of the sound level in decibels calculated over 5 s

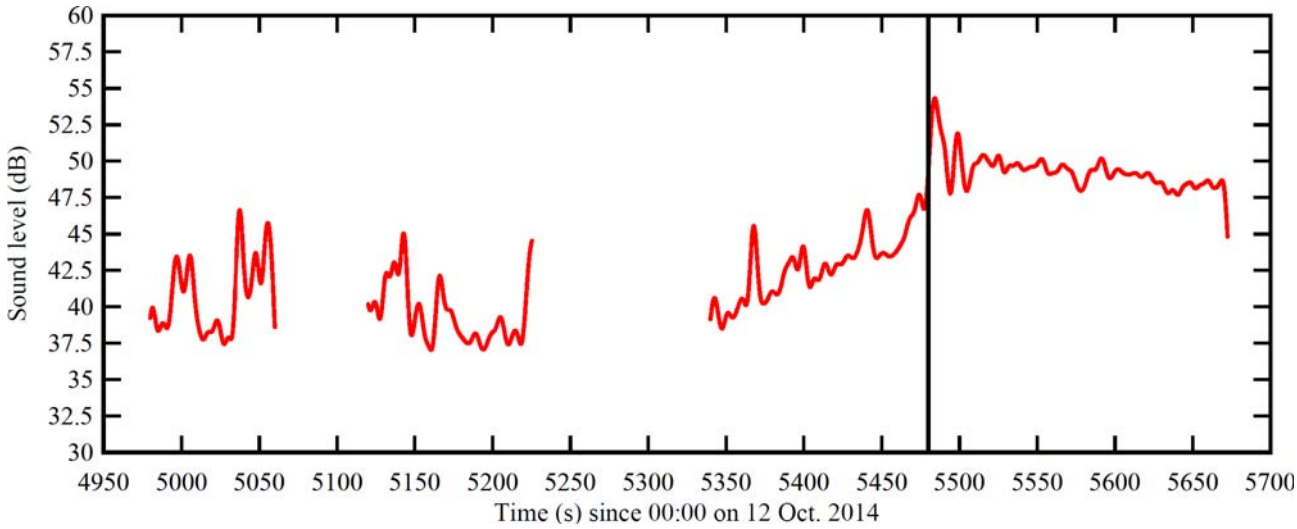

CHANSON, H. (2016). "Atmospheric Noise of a Breaking Tidal Bore." *Journal of the Acoustical Society of America*, Vol. 139, No. 1, pp. 12-20 (DOI: 10.1121/1.4939113) (ISSN 00014966).

Fig. 5 - Sound pressure acoustic spectra of the tidal bore event, Qiantang River bore at Yanguan on 12 October 2015 between 01:22 and 01:42 - Average of left and right sound track spectra, tidal bore passage in front of microphone: t = 5634 s, first period: t < 5480 s, second period: t > 5480 s

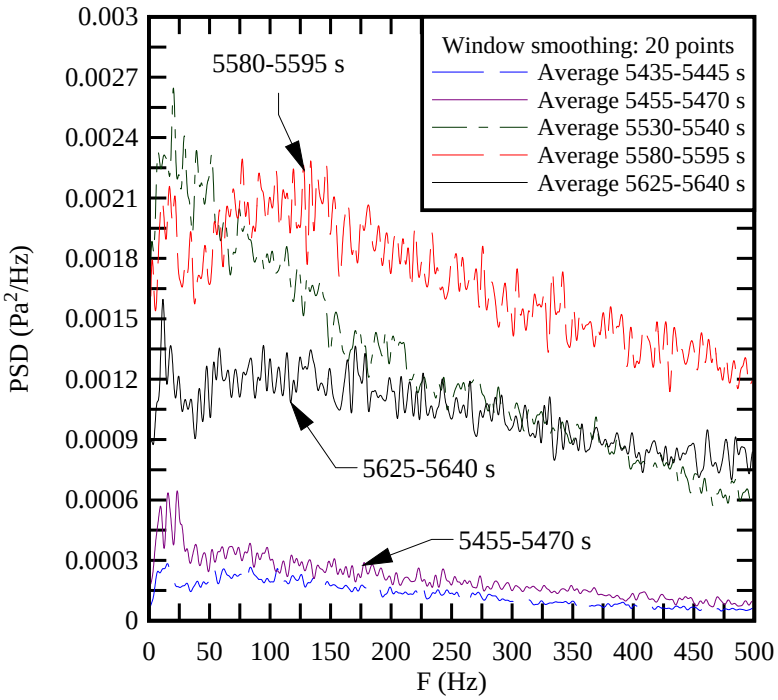

CHANSON, H. (2016). "Atmospheric Noise of a Breaking Tidal Bore." *Journal of the Acoustical Society of America*, Vol. 139, No. 1, pp. 12-20 (DOI: 10.1121/1.4939113) (ISSN 00014966).

Fig. 6 - Acoustic spectra of the laboratory breaking bore - Average of left and right sound track spectra, Run 1

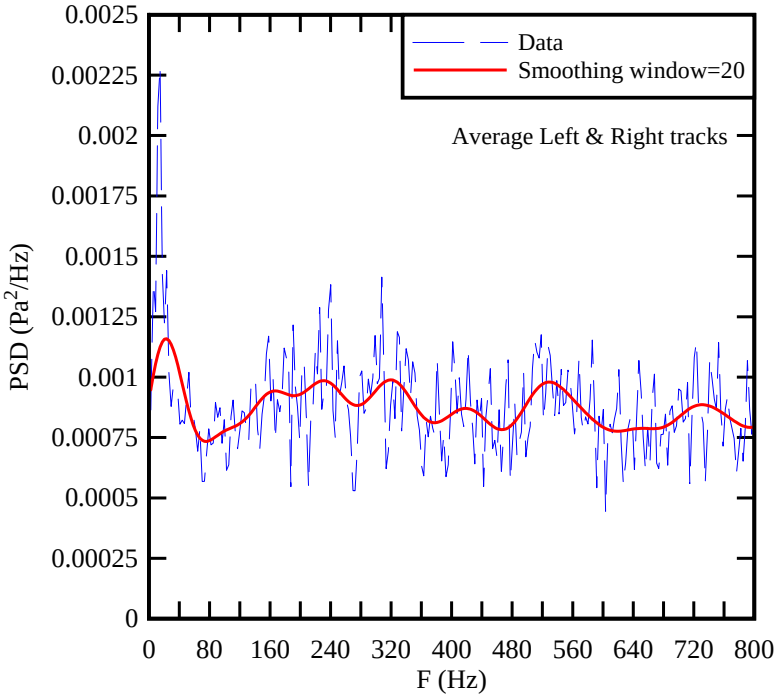

Fig. 7 - Dimensionless aeration length in breaking bores (Present laboratory study) and stationary hydraulic jumps (HJ) (Rajaratnam 1962, Chanson 2010)

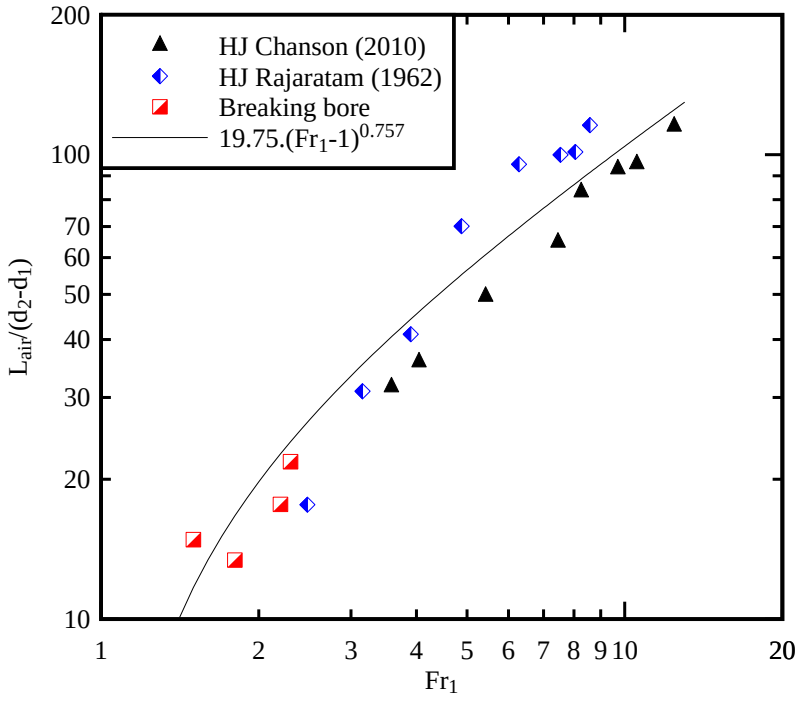

Fig. 8 - Three-dimensional sketch of a breaking tidal bore roller

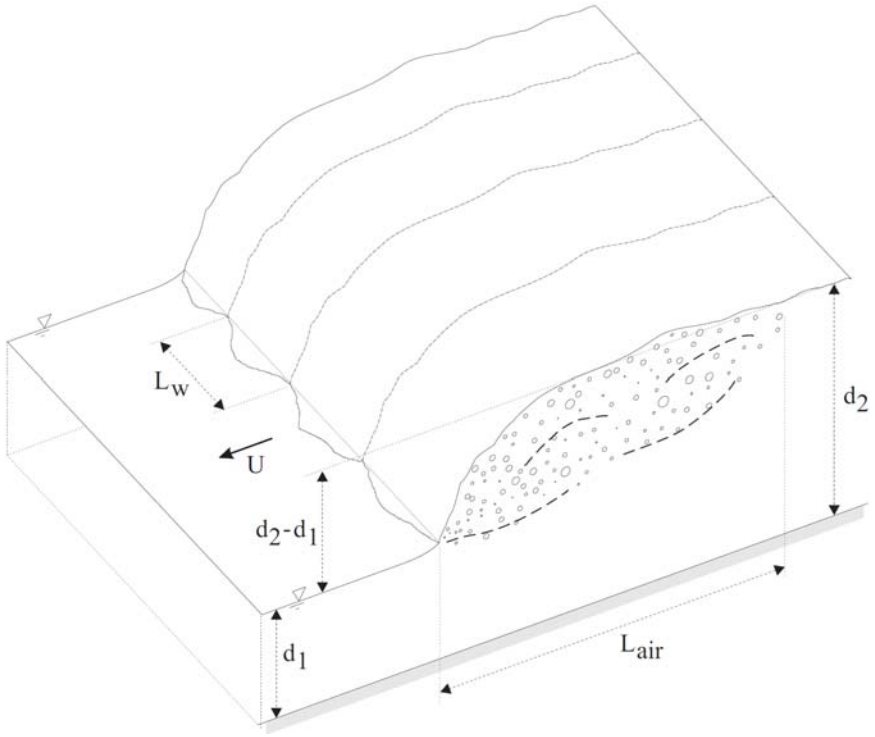

Fig. 9 - Dominant rumble sound frequencies generated by breaking tidal bores as functions of the bore roller perimeter wave length L_w - Comparison with Equation (4)